A Quantitative Resolution of Overlapped Chromatographic Fractions by Target Transformation Factor Analysis

Ihn Chong Lee†, Seungwon Kim, Chul Lee*, and Sang Won Choi‡

Department of Chemistry, Hanyang University, Seoul 133-791
†Department of Chemistry, Hallym University, Chuncheon 200-702
‡Department of Chemical Engineering, National Fisheries University of Yosu, Cheonnam 550-749. *Received January 25, 1991*

Target transformation factor analysis is applied to analyze the components of unresolved fraction in the elution curve of La, Pr and Gd which is obtained using the chelate agent- impregnated resin and 0.7 M hydrochloric acid as an eluent. We determined the number of components contributing to the unresolved fractions and verified the presence of suspected components.

Introduction

The problem of curve resolution in chromatography is important in analytical chemistry as well as in the practical separation of metals. All qualitative and quantitative analyses and the estimation of metal purities in the separation processes that use chromatography rely on the pure peaks.

Since the first application of factor analysis (FA), a computer techniques for solving multidimensional problems, performed curve resolution,[1] it has been successfully applied to resolve overlapped peaks in gas chromatography-mass spectrometry (GC-MS) data,[2,3] and liquid chromatography-ultraviolet (LC-UV) data.[4,5]

In one approach of spectral information using multivariate techniques, the wavelength and absorbance information from a large spectral segments have been used for a number of different samples, consisting of both standards and unknowns, with each wavelength giving a discrete absorbance measurement. Factor analysis is applied directly to this spectral information then gives the number of components and their concentrations without the need for concern about spectral overlaps and interferences.[6,7] Such direct factor analysis has not been previously attempted for the curve resolution of column chromatographic spectra in the separation process. In the present investigation, FA is carried out on the visible spectral data obtained in the column separation process which consists of the combination of a chelate agent-impregnated resin and a mineral acid as an eluent.

Basis

Principal Component Analysis. Abstract factor analysis (AFA) and target transformation factor analysis (TTFA) are used to determine the number of components and verify individually the presence of suspected components contributing to the unresolved column chromatographic peak.

In the case of column chromatography, a raw data matrix, $[A]_{raw}$ is the absorbances of effluents measured at regular intervals as time or volume. Successive rows in $[A]_{raw}$ are acquired over a period of time during which a cluster of elution peaks is observed. Each column in $[A]_{raw}$ corresponds to the chromatogram one would obtain using a single-wavelength detector. The total absorbances due to n components measured at time i and wavelength j A_{ij}, is factor-analyzable provided that as expressed in Eq. (1). Each of absorbances is a linear sum of contributions from individual components obeying Beer's law[8]

$$A_{ij}=b\sum_{k=1}^{n}(c_{ik}\ e_{kj}) \tag{1}$$

where b is the path length of cell, c_{ik} is the concentration of component k during time i and e_{kj} is the molar absorptivity of component k at wavelength j. The matrix from of Eq. (1) becomes

$$\underset{i\times j}{[A]_{raw}}=b\underset{i\times n}{[C]}\ \underset{n\times j}{[E]} \tag{2}$$

where $[A]$ is the $i\times j$ matrix of absorbance data at i scans and j wavelengths for n components, $[C]$ is the $i\times n$ matrix of concentration and $[E]$ is the $n\times j$ matrix of the pure absorptivity. Each column of $[C]$ represents the concentration profile of one component while the corresponding row of $[E]$ represents the spectrum of that pure component. Ordinarily, the wavelengths are equally spaced. To ensure a high degree of statistical accuracy both the number of rows and columns in the data matrix must exceed n by at least 2.

AFA can be used to determine both the number and identities of the components contributing to the unresolved peak. AFA, the first step in TTFA, decomposes the data matrix into abstract factors. To accomplish this task FA makes use of the covariance matrix. The covariance matrix $[Z]$ is calculated according to Eq. (3).

$$[Z]=[A]_{raw}\ [A]^{T}_{raw} \tag{3}$$

where $[A]^{T}_{raw}$ is the transposed matrix of $[A]_{raw}$. Throughout this work the covariance about the origin has been used. The covariance matrix is then decomposed by the method of principal component analysis[9] to produce the set of n principal eigen vectors $[Q]_n$ and the corresponding eigenvalues λ_n:

$$[Q]_n^{-1}[Z][Q]_n=[\lambda_i\ \delta_{ik}] \tag{4}$$

where δ_{ik} is the well-known Kronecker delta

$$\delta_{ik}=\begin{cases}0 & \text{if } i\neq k\\ 1 & \text{if } i=k\end{cases} \tag{5}$$

Here, λ_i is an eigenvalue of the set of equation having the following form:

$$[Z]\cdot\{Q\}_i=\lambda_i\cdot\{Q\}_i \tag{6}$$

where $\{Q\}_i$ is the ith column of matrix $[Q]_n$. These columns form an orthonormal set. In reality the diagonalization matrix, $[Q]_n$ is a valid representation for the absorptivity matrix $[E]$[10]:

$$[E]_{abst}=[Q]_n^T \tag{7}$$

The concentration matrix is given:

$$[C]_{abst}=[A]_{raw}\cdot[Q]_n \tag{8}$$

The resulting matrices are abstract absorptivity and concentration matrices as expressed in Eq. (7) and (8) and are used to construct a linear model which can be used to reproduce the original raw data.

The eigenvector analysis itself gives the number of components, *i. e.*, the number of elements, present in an unknown. There are numerous methods for determining the cutoff between significant eigenvectors (the number of components) and the residual eigenvectors (random noise in the spectra).

The theory gives three types of error, *i.e.*, real error (*RE*), imbedded error (*IE*) and extracted error (*XE*). These errors are estimated according to Eq. (9)-(11).

$$RE=\left(\sum_{i=n+1}^{x}\lambda_i/y\cdot(x-n)\right)^{1/2} \tag{9}$$

$$XE=\left(\sum_{i=n+1}^{x}\lambda_i/y\cdot x\right)^{1/2} \tag{10}$$

$$IE=[(RE)^2-(XE)^2]^{1/2} \tag{11}$$

where x is the number of rows or columns in $[A]_{raw}$, whichever is smaller; y is the number of rows or columns whichever is larger.

In this work x is the number of scans (rows) in $[A]_{raw}$ and y is the number of wavelengths (colums) in $[A]_{raw}$. n represents the number of factors, *i.e.*, elements, used to reproduce the data, and λ_i is the i-th eigenvalue of $[A]_{raw}$.

Among the error functions, *RE* method depends upon an accurate estimate of the error. In many real chemical problems, such information is difficult to obtain and is not available in this work. Therefore, *IE* function has been used in this work. By studying the behavior of the *IE* as a function of n, the size of the true factor space n_c as well as the error in the data can be deduced without recourse to any a prior knowledge of the error. The point at which the IE function reaches a minimum corresponds to the factor space, n_c.

IND function, an empirical function in nature, as shown in Eq. (12) is given by Malinowski to reach a minimum when the correct number of factors are employed.

$$IND=RE/(x-n)^2 \tag{12}$$

The remaining number of eigenvectors, n_c, also called abstract factors, span the same space spanned by real factors (the concentrations of the elements present in the solutions) but do not correspond with them. A coordinate transformation from abstract space to a real factor space where each axis corresponds directly to the concentration of one element is desired.

Target Transformation. Target transformation as well as identification of one or more of the suspected factors involves using the abstract row matrix.[6] The suspected factors are represented by a test matrix $[C]_{test}$. The test matrix is constructed which contains the known concentration (or absorbance) of the standards and has the dimensions $(x\times n_c)$ where x is the number of standards (or the number of fractions) used to generate $[A]$ and n_c is the number of component to be determined.

The transformation matrix $[T]$ is calculated according to Eq. (13).

$$\underset{n_c\times n_c}{[T]}=\underset{n_c\times x}{[C]_{abst}^T}\ \underset{x\times n_c}{[C]_{test}} \tag{13}$$

where $[C]_{abst}^T$ is the transposed matrix of $[C]_{abst}$. The transformation matrix from Eq. (13) can be used to calculate the fitted or predicted concentration according to Eq. (14).

$$\underset{x\times n_c}{[C]_{pred}}=\underset{x\times n_c}{[C]_{abst}}\ \underset{n_c\times n_c}{[T]} \tag{14}$$

The residuals of the fit in the concentration vector space can be used to estimate the standard deviation of the predicted concentration by Eq. (15).

$$Sn^2=\sum_{i=1}^{x}(c_{pred,i}-c_{test,i})^2/(x-n_c) \tag{15}$$

where Sn is the standard deviation of predicted concentration of n-th component; $c_{pred,i}$ and $c_{test,i}$ are the predicted and actual concentrations or absorbances of the n-th component at the i-th scan respectively; x is the number of scans.

Unknown Calculation. The procedure outlined below is similar to that described by Gemperline *et al.*.[6] The absorption spectra of x effluents are measured at the y wavelengths as described above. These spectra are then used to form x rows in a raw data matrix of unknown samples, $[A]_{samp}$. In order to calculate the unknown concentrations of the x effluents, the data matrix, $[A]_{samp}$ was projected into n_c concentrations space according to Eq. (16).

$$\underset{n_c\times x}{[C]_{proj}^T}=(\underset{n_c\times y}{[E]_{abst}}\ \underset{y\times n_c}{[E]_{abst}^T})^{-1}\underset{n_c\times y}{[E]_{abst}}\ \underset{y\times x}{[A]_{samp}^T} \tag{16}$$

Eq. (16) may be simplified to give Eq. (17), where $[\lambda]^{-1}$ is the inverse of the matrix of eigenvalues obtained from the principal component analysis.

$$\underset{n_c\times x}{[C]_{proj}^T}=\underset{n_c\times n_c}{[\lambda]^{-1}}\ \underset{n_c\times y}{[E]_{abst}}\ \underset{y\times x}{[A]_{samp}^T} \tag{17}$$

The transformation matrix $[T]$, calculated by Eq. (13), can be used to predict the concentration in the effluent fractions:

$$\underset{x\times n_c}{[C]_{samp}}=\underset{x\times n_c}{[C]_{proj}}\ \underset{n_c\times n_c}{[T]} \tag{18}$$

In this equation, each row of $[C]_{samp}$ contains the predicted concentrations of n components in the corresponding effluents.

Experimental

A combination of solvent extraction and ion exchange is considered one of ideal methods for the column separation to obtain highly purified rare earths. Suzuki *et al.* proposed

Table 1. Compositions of Various Solutions (M)

Solutions	La	Pr	Gd
1	0.054	0.027	0.024
2	0.108	0.0	0.0
3	0.0	0.106	0.0
4	0.0	0.0	0.095
5	0.049	0.011	0.037

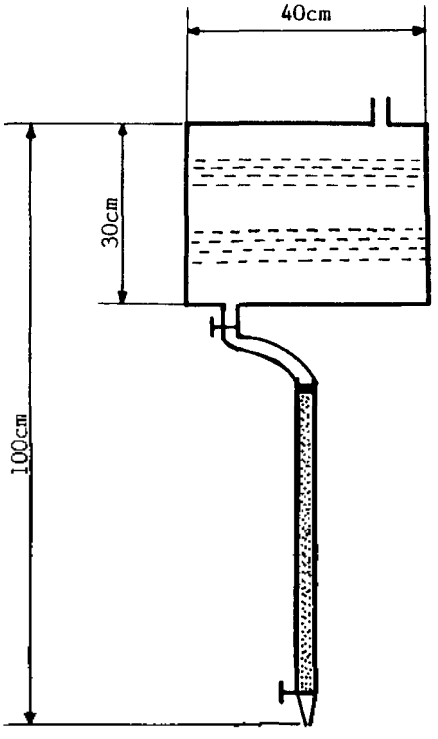

Figure 1. A column (10 mmΦ×500 mmL) for the separation of rare earths using D2EHPA-impregnated Amberlite XAD-7.

to use an ion selective resin as a stationary phase which can readily be prepared by impregnation of chelate extractants such as di(2-ethylhexyl) hydrogen phosphate (D2EHPA) and 2-ethylhexyl hydrogen 2-ethylhexylphosphonate (PC-88 A) into porous polymer beads.[11]

The present works carried out to separate the individually rare earth metals using D2EHPA-impregnated XAD-7 polymer and diluted hydrochloric acid as an eluent. The chromatographic overlaps were so severe that an attemp was tried to resolve them by TTFA. Three elements such as La, Pr and Gd, which were found to be severely interfered, were selected for the study in the present investigation.

Reagents. The D2EHPA was obtained from TCI, Japan and used as received. Stock solutions of the elements were prepared by dissolving the corresponding oxides (99.9% Aldrich Chemical Co) into 0.5 m*l* volume of 4 N hydrochloric acid. The compositions of the solutions are given in Table 1. 1st and 5th solutions were synthesized and used as a mixed standard and a mixed sample solution, respectively. The three single-solute solutiolns were made and used as respective test-vector solutions. Other chemicals were of reagent grade and were used with no further purification.

Resin bead. Amberlite XAD-7 (20-60 mesh) was obtained from Sigma Chemical Co. and used as the polymer support. Resin beads were washed successively with diluted nitric acid and acetone and then dried in vacuum prior to use. A 5.25 m*l* volume of D2EHPA was diluted with 30 m*l* of acetone. To this solution was added a 5 g portion of the XAD-7 beads and the mixture was stirred under the reduced pressure. After 30 min, the acetone was evaporated off. The obtained resin contains 50% (w/w) of D2EHPA. Packed column was prepared generally as described elsewhere.[12] Leaking of D2EHPA from the resin is practically negligible.

Table 2. Chromatographic Operation Conditions

Packing material: D2EHPA impregnated Amberlite XAD-7
Size of column: 10 mmΦ×500 mmL
Loading volumn: 1 m*l*
Mobile phase: 0.7 M HCl
Flow rate: 1.0 m*l*/min
Total amount of metals: 15 mg
Detector: UV-Vis., path length of cell: 10 mm
Color developing agent: Methyl thymol bule (MTB)

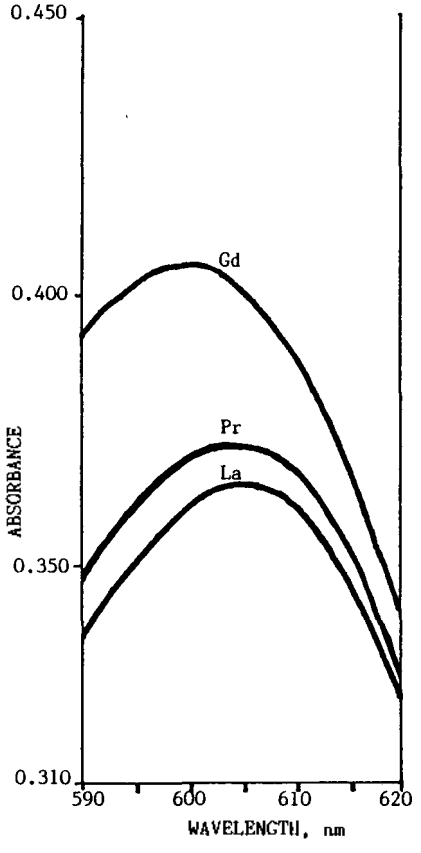

Figure 2. Typical absorbance spectra of La, Pr and Gd.

Procedure. A chromatographic separation of La(III), Pr (III) and Gd(III) was carried out using a resin column as shown in Figure 1. The volume of the eluent reservoir was kept large so as to obtain a constant flow rate. The chromatographic operating conditions are presented in Table 2.

The effluents were received in 10 m*l* at the exit of the column. Each fraction of 10 m*l* was collected carefully to the meniscus of 10 m*l* measuring flask and 11 fractions were all.

Table 3. Absorbances of Chromatographic Fractions Measured at 605 nm

Solutions \ Fractions	1	2	3	4	5	6	7	8	9	10	11
1	.1498	.3554	.3323	.3292	.3111	.2996	.3145	.3052	.2979	.2799	.2162
2	.2872	.5438	.5155	.4467	.3024	.1500	.0661	.0338	.0202	.0132	.0118
3	.1603	.4679	.4570	.4562	.4303	.4177	.3736	.2682	.1786	.1375	.0403
4	.0000	.0223	.1071	.2981	.4934	.5748	.5928	.5927	.5863	.5248	.4234
5	.1587	.3135	.2898	.2520	.2745	.2879	.2977	.3269	.3152	.3112	.2409

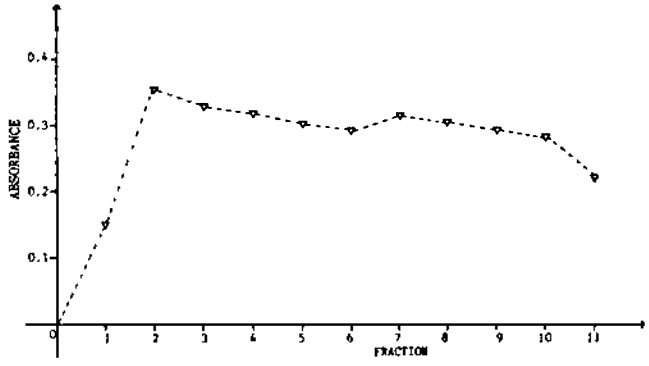

Figure 3. A chromatogram of fractions of the mixed standard solution measured at 605 nm.

From each of the effluent fractions of 10 m*l*, an accurate 5 m*l* volume was transferred into the measuring flask of 50 m*l*. To this flask, 2.0 m*l* volume of 0.05% methyl thymol blue (MTB) solution was added as the color developing agent. For making the MTB solution, a 0.01 g of MTB was dissolved in a mixture of 18 m*l* of distilled water and 2.0 m*l* of the 20% aqueous solution of hexamethylenetetraamine.[13]

The solution in the measuring flask of 50 m*l* was adjusted to pH 6.5 with an diluted ammonia solution. The solution was diluted with distilled water to the meniscus.

For each fraction, 31 absorbance values were obtained at 1 nm intervals from 590 to 620 nm using Hitach model U-3200 UV-visible spectrophotometer with the bandwidth at 0.5 nm. Silica cells of 1 cm were used. The sample cells containing the appropriate fractions of the mixed standard and sample solutions or test vector solutions were added. The reference cell contained 0.7 M HCl mobile phase which had been treated samely as described above for sample solutions. Typical recorded spectra of three test vector solutions are given in Figure 2.

The elution curve for the mixed standard solution was obtained by measuring the absorbances of effluents at 605 nm, corresponding with maximum absorptivity(Table 3). The curve was tailed as shown in Figure 3 and the tailing component was found to be only Gd. With the present operation condition, the elution curve was so reproducible that the cut off at 11 fractions did not given any erratic results on TTFA. The elution curves of three test vector solutions would be similarly obtained. The absorbances are in Table 3 and used in place of concentrations for target test on TTFA.

Results and Discussion

Table 4. Results of Abstract Factor Analysis Using the Mixed Standard Solution

n	Eigenvalue	*RE*	*XE*	*IE*	$IND \times 10^5$
1	83.42612	0.00309	0.00295	0.00092	3.090
2	0.00231	0.00153	0.00138	0.00066	1.884
3	0.00061	0.00040	0.00034	0.00021	0.628
4	0.00001	0.00037	0.00030	0.00021	0.759
5	0.00001	0.00033	0.00024	0.00021	0.911
6	0.00001	0.00025	0.00017	0.00018	1.016

The absorbances were factor-analyzed as described below by the computer program "FA" which was developed in this laboratory. The program allows for either reduced or full output for both AFA and TTFA.

A 11-row by 31-column data matrix $[A]_{raw}$ was formed from the absorbances at the 31 wavelengths of the 11 fractions of the mixed standard solution, *i.e.*, solution 1 in Table 1. This matrix was subjected to AFA. The theory of error for AFA was applied in order to determine the number of component n_c, *i.e.*, the number of factors. This involved evaluating the *RE*, the *IE* and the *IND* by means of Eq. (9) to 12, using $n=1$ to $n=6$ factors to reproduce the data (see Table 4). The numbers of rows and columns in the data matrix, the eigenvalues and n were needed to this quantity.

The *RE* method depends upon an accurate estimate of the experimental errors. Such information is not available in the present work. Therefore, *IE* and *IND* were used. The presence of three factors, *i.e.*, $n=n_c=3$, is indicated by the IE, since this function did not decrease appreciably beyond $n=3$ and is much smaller at $n=3$ than at $n=2$ (Table 4). The *IND* values for data matrix $[A]_{raw}$ also reached a minimun at the $n=3$. These are consisted with the known presence of three absorbing components, *i.e.*, $n=n_c=3$, in solution 1 in Table 1.

Test vectors of three single-solute solutions were constructed from absorbances of 11 fractions(Table 3) measured at 605 nm. Target tests of three test vectors were carried out on the data matrix $[A]_{raw}$ according to Eq. (13) and (14) using three factors. Absorbance plots of the resulting TTFA-predicted absorbances are shown in Figure 4.

A quantitative measure of the differences between the experimental absorbances given in Table 3 and the predicted absorbances given in Figure 4 is provided by the calculation of the residuals explained in Eq. (15). Inspection of the residuals for individual fractions showed a reproducible bias. The residuals were all of the same order of magnitude and

Table 5. The Results Predicted from Three Single-Solute Solutions by Target Testing

Single-solute solutions	Known concentration (M)	Predicted concentration (M)	Standard deviation, S_n	Standard deviation (M)	Deviation in percentage
2	0.108	0.110	0.0598	0.003	2.51
3	0.106	0.109	0.1287	0.004	3.70
4	0.095	0.092	0.1771	0.004	4.22

Table 6. A Comparison of Calculated or Predicted with Known Concentrations(M)

Elements / Solutions	La				Pr				Gd			
	Known	Pred.	Calc.	Dev.(%)	Known	Pred.	Calc.	Dev.(%)	Known	Pred.	Calc.	Dev.(%)
1	0.054	0.053		1.51	0.027	0.025		6.88	0.024	0.026		8.37
5	0.049		0.048	3.01	0.011		0.010	7.38	0.037		0.039	4.28

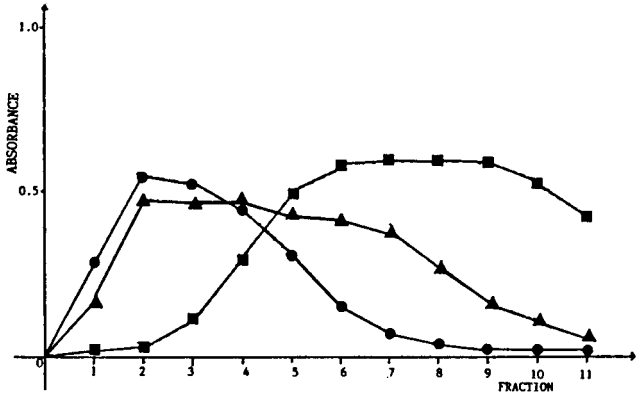

Figure 4. Predicted curves obtained from three single-solute solutions by target testing. (●: La, ▲: Pr, ■: Gd).

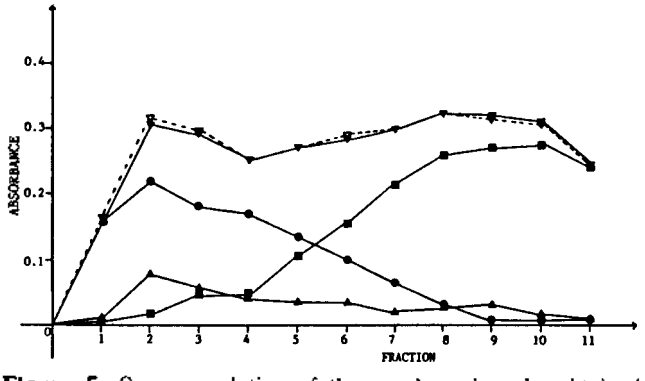

Figure 5. Curve resolution of the overlapped peaks obtained from the mixed sample solution. (●: La, ▲: Pr, ■: Gd, ▽ and ▼: tota, ------: experimental, —: calculated).

did not appear to show evidence of any consisted bias. The standard deviations given by Eq. (15) were calculated and given in Table 5. The relatively small deviations indicate the presence of the three components.

Sample solution matrix $[A]_{samp}$ was similarly made from the mixed sample solution(sample 5 in Table 1) as for the data matrix $[A]_{raw}$ for AFA. The 11 absorbances of each component at the wavelength of maximum absorptivity, *i.e.*, at 605 nm, were calculated according to Eq. (16) to Eq. (18). The resolved curve is given in Figure 5. The sum of absorbances of 11 fractions was compared with the corresponding sum from each test vector solution to calculate each elemental concentration. The calculated results are given in Table 6. The data matrix $[A]_{raw}$ was used again in place of $[A]_{samp}$ to predict the concentration of each element in the mixed standard solution. The predicted concentrations are also given in Table 6.

The small differences between the known concentrations and calculated or predicted concentrations indicat that the combined techniques of AFA and TTFA can serve to resolve such a column chromatographic curve as that of present work.

Acknowledgement. This work was carried out with the financial assistance from the Korea Science and Engineering Foundation, 1989, Project No. KOSEF 87-0309-09, and the Basic Science Research Institute Program, Ministry of Education, 1990, Project No. BSRI-90-130.

References

1. W. H. Lawton and E. A. Sylvester, *Technometrics*, **13**, 617 (1971).
2. D. Macnaughtan, L. B. Rogers and G. Wernimont, *Anal. Chem.*, **44**, 1421 (1972).
3. B. R. Kowalski and M. A. Sharaf, *Anal. Chem.*, **54**, 1291 (1982).
4. B. R. Kowalski and D. W. Osten, *Anal. Chem.*, **56**, 991 (1984).
5. P. J. Gemperline, *J. Chem. Inf. Comput. Sci.*, **24**, 206 (1984).
6. P. J. Gemperline, S. E. Boyette and K. Tyndall, *Appl. Spectrosc.*, **41**, 454 (1987).
7. P. J. Gemperline, *Anal. Chem.*, **58**, 2656 (1986).
8. M. McCue and E. R. Malinowski, *Appl. Spectrosc.*, **37**, 463 (1983).
9. E. R. Malinowski and D. G. Howery, "Factor Analysis in Chemistry", John Wiley and Sons, New York, 1980.

10. E. R. Malinowski, *Anal. Chem.*, **49**, 606 (1977).
11. Y. Wakui, H. Matsunaga and T. M. Suzuki, *Anal. Sci.*, **4**, 325 (1988).
12. M. B. Colella, S. Siggia and R. M. Barns, *Anal. Chem.*, **52**, 2347 (1980).
13. K. W. Cha, E. S. Jung and J. H. Lee, *J. Kor. Chem. Soc.*, **33**, 304 (1989).

Equilibrium and Non-equilibrium Molecular Dynamics Simulations of Thermal Transport Coefficients of Liquid Argon

Chang Bae Moon, Gyeong Keun Moon, and Song Hi Lee*

Department of Chemistry, Kyungsung University, Pusan 608-736. *Received January 29, 1991*

The thermal transport coefficients-the self-diffusion coefficient, shear viscosity, and thermal conductivity-of liquid argon at 94.4 K and 1 atm are calculated by non-equilibrium molecular dynamics (NEMD) simulations of a Lennard-Jones potential and compared with those obtained from Green-Kubo relations using equilibrium molecular dynamics (EMD) simulations and with experimental data. The time-correlation functions-the velocity, pressure, and heat flux auto-correlation functions-of liquid argon obtained from the EMD simulations show well-behaved smooth curves which are not oscillating and decaying fast around 1.5 ps. The calculated self-diffusion coefficient from our NEMD simulation is found to be approximately 40% higher than the experimental result. The Lagrange extrapolated shear viscosity is in good agreement with the experimental result and the asymptotic formula of the calculated shear viscosities seems to be an exponential form rather than the square-root form predicted by other NEMD studies of shear viscosity. The agreement for thermal conductivity between the simulation results (NEMD and EMD) and the experimental result is within statistical error. In conclusion, through our NEMD and EMD simulations, the overall agreement is quite good, which means that the Green-Kubo relations and the NEMD algorithms of thermal transport coefficients for simple liquids are valid.

Introduction

Molecular theory of transport through gases and liquids is now very active area of research and it has been only in the 1960s that this field has been set on a basis comparable to equilibrium statistical mechanics. There are various theories of transport in gases and liquids: the elementary kinetic theory of gases and molecular collisions, the macroscopic equations of continuum mechanics or hydrodynamics such as the continuity equation, the momentum balance equation, and the energy balance equation (this is essentially the thermodynamic background for non-equilibrium statistical mechanics), the concept of phase space and Liouville equation which result in the reduced distribution function and BBGKY hierarchy for fluid distribution function, the Boltzmann equation and the Chapman-Enskog method which are respectively the central equation of the rigorous kinetic theory of gases and the standard method for solving this Boltzmann (integrodifferential) equation, and finally the time-correlation function method (Green-Kubo relations) which is probably the most successful theory for transport of liquids.

Green and Kubo[1] showed that the phenomenological coefficients describing many transport processes and time-dependent phenomena in general could be written as integrals over a certain type of function called a time-correlation function. These time-correlation functions play a somewhat similar role in nonequilibrium statistical mechanics that the partition function plays in equilibrium statistical mechanics. The analogy breaks down in one respect. Since the state of thermal equilibrium is unique, a single partition function gives all the thermodynamic properties, but since there are many different kinds of nonequilibrium states, a different time-correlation function for each type of transport process is needed. Determining the appropriate time-correlation function to use for a particular transport process of interest is very important.

The Green-Kubo relations (Table 1) are the formal expres-

Table 1. Green-Kubo Relations for Thermal Transport Coefficients

$$D_s = \frac{1}{3}\int_0^\infty dt\,\langle v_i(0)\cdot v_i(t)\rangle \quad \text{self-diffusion coefficient} \tag{1}$$

$$\eta = \frac{V}{kT}\int_0^\infty dt\,\langle P_{xy}(0)P_{xy}(t)\rangle \quad \text{shear viscosity} \tag{2}$$

$$\lambda = \frac{V}{kT^2}\int_0^\infty dt\,\langle J_{Qx}(0)J_{Qx}(t)\rangle \quad \text{thermal conductivity} \tag{3}$$

where v_i is the velocity of particle i, P_{xy} is an off-diagonal ($x \neq y$) of the viscous pressure tensor:

$$PV = \sum_i mv_iv_i + \sum_i r_iF_i \tag{4}$$

and J_{Qx} is a component of the energy current:

$$J_Q V = \sum_i E_i v_i + \frac{1}{2}\sum_i\sum_j r_{ij}(v_i \cdot F_{ij}) \tag{5}$$